**Chemistry of Metals and Alloys**

*Chem. Met. Alloys* 17 (2024) 58-62
Ivan Franko National University of Lviv
http://publications.lnu.edu.ua/chemetal

# $NdNiIn_{1-x}Sn_x$ solid solutions at 870 K

Galyna NYCHYPORUK[1]*, Myroslava HORIACHA[1,2], Oleh HUDZO[1], Vasyl ZAREMBA[1]

[1] *Department of Inorganic Chemistry, Ivan Franko National University of Lviv, Kyryla i Mefodiya St. 6, 79005 Lviv, Ukraine*
[2] *Leibniz Institute for Solid State and Materials Research (IFW) Dresden, Helmholtz Str. 20, 01069 Dresden, Germany*
* *Corresponding author. Tel.:* +380-32-2394483*; e-mail: halyna.nychyporuk@lnu.edu.ua*

Received October 11, 2024; accepted December 17, 2024
https://doi.org/10.30970/cma17.0449

**The interaction between the components in the NdNiIn–NdNiSn system was investigated by X-ray powder diffraction, scanning electron microscopy, and energy-dispersive X-ray spectroscopy in the full concentration range at 870 K. The formation of two substitutional solid solutions was observed: $NdNiIn_{1.0-0.6}Sn_{0-0.4}$ (ZrNiAl-type structure; space group *P*-62*m*; *a* = 0.75375(9)-0.74694(6), *c* = 0.39359(6)-0.39624(4) nm) and $NdNiSn_{1.0-0.9}In_{0-0.1}$ (TiNiSi-type structure; space group *Pnma*; *a* = 0.73959(9)-0.74212(10), *b* = 0.45438(5)-0.45588(6), *c* = 0.76754(9)-0.76984(11) nm). The partial replacement of indium atoms by tin atoms in NdNiIn was confirmed by single-crystal X-ray diffraction and EDX data. $NdNiIn_{0.6}Sn_{0.4}$ crystallizes with ZrNiAl-type structure (*P*-62*m*, *hP*9, *a* = 0.74689(2); *c* = 0.39483(1) nm, $R_1$ = 0.0202, $wR_2$ = 0.0477).**

**Indium / Solid solution / X-ray powder diffraction / Single crystal / Crystal structure**

## 1. Introduction

NdNiIn and NdNiSn are representatives of a large group of ternary compounds with the equiatomic composition *RTM* (*R* = rare earth, *T* = transition metal, *M* = *p*-element) [1-5]. They are being studied quite intensively due to a number of interesting physical properties such as Kondo effect, superconductivity, spin fluctuations, valence instability and the behavior of heavy fermions, magnetic transitions, metamagnetism, *etc.* [6-14]. The Nd*T*In compounds are ferromagnetic for *T* = Ni and Pd, antiferromagnetic for *T* = Cu, and paramagnetic for *T* = Au [9]. The compound NdNiSn orders antiferromagnetically with a Néel temperature ($T_N$) of about 3 K. It has been studied by various approaches: crystal structure, magnetic susceptibility, heat capacity, X-ray photoemission spectroscopy, neutron diffraction, *etc.* [12,13]. The compounds LaNiSn and NdNiSn and their deuterides have been studied using $^{119}$Sn Mössbauer spectroscopy with variable temperature. The compound NdNiSn, which is nonmagnetic above 12.5 K, exhibits magnetic ordering below 25 K after deuteration, while the compound LaNiSn and its deuteride do not exhibit magnetic ordering above 4.2 K [14].

It was found that in the similar quasi-binary systems NdNiIn–NdCuIn and NdNiIn–NdNiAl, the formation of a continuous solid solution with a structure of the ZrNiAl type is observed, and in the case of substitution of Al for In, the solubility range is limited to the region NdNiIn–$NdNiIn_{0.75}Al_{0.25}$. This pattern is also observed for the hydrides [15]. Ardeleani *et al*. [16] studied the $PrNiIn_{0.8}Sn_{0.2}$ and $NdNiIn_{0.8}Sn_{0.2}$ phases to observe the influence of the rare-earth metal on the stability of the hydride, and showed that at 3 MPa they have the compositions $PrNiIn_{0.8}Sn_{0.2}H_{1.33}$ and $NdNiIn_{0.8}Sn_{0.2}H_{1.26}$, respectively.

The aim of this work was to study the interaction of the components in the NdNiIn–NdNiSn system in the full concentration interval at 870 K.

## 2. Experimental details

Polycrystalline samples (up to 1 g) in the $NdNiIn_{1-x}Sn_x$ system, where *x* ranges from 0 to 1.0 with steps of 0.1, were prepared by arc melting of the pure elements (all with stated purities better than 99.8%) under an argon atmosphere of *ca*. 800 mbar, purified using titanium sponge. Homogeneity of the alloys was achieved by annealing in evacuated quartz ampoules in an electric SNOL muffle furnace with automatic temperature control (±2 K) for 30 days at a temperature of 870 K. The alloys were hardened in cold water without previously breaking the ampoules. The samples were stable in air in both bulk polycrystalline and powder

forms. The samples were analyzed by powder X-ray diffraction using DRON 2.0M (Fe *K*α radiation) and STOE STADI P (Cu $K\alpha_1$ radiation) diffractometers. Phase analysis was performed using Powder Cell [17] and STOE WinXPOW [18] software. Structural refinements were performed using the Fullprof package [19]. Some alloys were examined on a Tescan Vega 3 LMU scanning electron microscope equipped with an Oxford Instruments SDD X-Max$^N$20 detector.

Single-crystal growth was performed by sealing the arc-melted sample with the starting composition $NdNiIn_{0.6}Sn_{0.4}$ ($Nd_{33.3}Ni_{33.3}In_{20}Sn_{13.4}$) in a small evacuated quartz ampule and heating it in a Naberterm HTCT 01/16 furnace. First, the sample was heated to 1173 K within 6 h and held at that temperature for 24 h, then cooled at a rate of 3 K $h^{-1}$ to 873 K and kept at that temperature for 6 h. Finally, the furnace was turned off. As a result, we could select irregularly shaped single crystals from the crushed alloy, and one of them was investigated on a SuperNova Rigaku Oxford Diffraction diffractometer (Mo *K*α radiation) at the Technical University of Dresden in order to check the crystal quality. Intensity data were collected at room temperature by using the same device. The crystal structure was refined using JANA 2006 software [20]. The qualitative and quantitative composition of single crystals was determined by EDX analysis (Zeiss EVO MA 15 scanning electron microscope) at the Leibniz Institute for Solid State and Materials Research (Dresden, Germany).

## 3. Results and discussion

The existence of two limited solid solutions of different lengths, based on the ternary compounds delimiting the NdNiIn–NdNiSn system, was observed during the investigation of the interaction between the components at 870 K. The limits of the solid solutions were determined according to the results of X-ray diffraction and EDX analysis (Fig. 1) and had the following unit-cell parameters: $NdNiIn_{1.0-0.6}Sn_{0-0.4}$ (ZrNiAl-type structure [21]; space group *P*-62*m*; *a* = 0.75375(9)-0.74694(6); *c* = 0.39359(6)-0.39624(4) nm) and $NdNiSn_{1.0-0.9}In_{0-0.1}$ (TiNiSi-type structure [22]; space group *Pnma*; *a* = 0.73959(9)-0.74212(10); *b* = 0.45438(5)-0.45588(6); *c* = 0.76754(9)-0.76984(11) nm). The unit-cell parameters of the ZrNiAl- and TiNiSi-type phases are given in Table 1. Some samples, in addition to the main phase, contained small amounts (up to 5 wt.%) of an impurity phase with $MgCu_4Sn$-type structure [23].

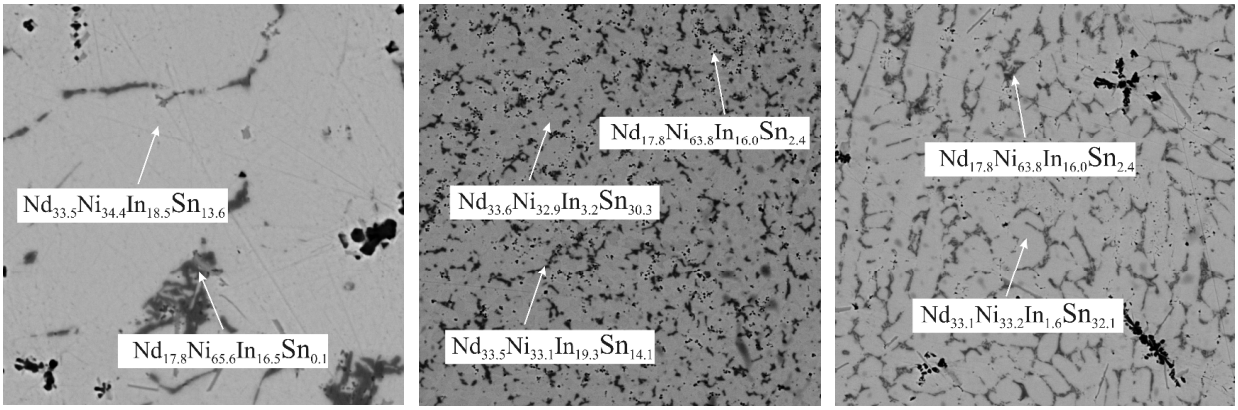


**Fig. 1** Back-scattered electron images of the surface of samples in the NdNiIn–NdNiSn system (samples annealed at 870 K): *a* – $NdNiIn_{0.7}Sn_{0.3}$, *b* – $NdNiIn_{0.4}Sn_{0.6}$, *c* – $NdNiIn_{0.2}Sn_{0.8}$.

**Table 1** Lattice parameters of samples within the solid solutions $NdNiIn_{1-x}Sn_x$.

| Sample | *a*, nm | *b*, nm | *c*, nm | *V*, nm$^3$ |
|---|---|---|---|---|
| $NdNiIn_{1-0.6}Sn_{0-0.4}$ (ZrNiAl-type, space group *P*-62*m*) | | | | |
| NdNiIn | 0.75375(9) | – | 0.39359(6) | 0.19366(4) |
| $NdNiIn_{0.9}Sn_{0.1}$ | 0.75240(8) | – | 0.39399(5) | 0.19316(4) |
| $NdNiIn_{0.8}Sn_{0.2}$ | 0.75038(8) | – | 0.39439(5) | 0.19232(7) |
| $NdNiIn_{0.7}Sn_{0.3}$ | 0.74901(6) | – | 0.39484(4) | 0.19184(3) |
| $NdNiIn_{0.6}Sn_{0.4}$ | 0.74694(6) | – | 0.39624(4) | 0.19145(3) |
| $NdNiIn_{0.1-0}Sn_{0.9-1}$ (TiNiSi-type, space group *Pnma*) | | | | |
| $NdNiIn_{0.1}Sn_{0.9}$ | 0.74212(10) | 0.45588(6) | 0.76984(11) | 0.26045(6) |
| NdNiSn | 0.73959(9) | 0.45438(5) | 0.76754(9) | 0.25794(5) |

The formation of a single-phase sample with composition $Nd_{0.33}Ni_{0.33}In_{0.20}Sn_{0.14}$ (STOE STADI P, Cu $K\alpha_1$ radiation, Fig. 2*a*) indicated the solubility of Sn in NdNiIn. Partial substitution of Sn atoms for In atoms was confirmed by a complete crystal structure determination (single-crystal method, automatic diffractometer Super Nova Rigaku Oxford Diffraction, Mo $K\alpha$ radiation, program JANA [20]): $NdNiIn_{0.6}Sn_{0.4}$, ZrNiAl-type structure [21]; space group *P*-62*m*; *hP*9, $a = 0.74689(2)$; $c = 0.39483(1)$ nm, $R_1 = 0.0202$, 494 $F^2$ values, 15 variables (Table 2). Indium and tin atoms form a statistical mixture, the composition of which was fixed according to the initial composition of the sample, in agreement with the results of the EDX analysis of a single crystal (33.8(1) at.% Nd: 33.6(1) at.% Ni: 19.3(1) at.% In: 13.3(1) at.% Sn) (Fig. 2*b*). The refined atomic coordinates of $NdNiIn_{0.6}Sn_{0.4}$ are listed in Table 3, interatomic distances and coordination numbers in Table 4, and the projection of the crystal structure onto the *ab* plane is shown in Fig. 3.

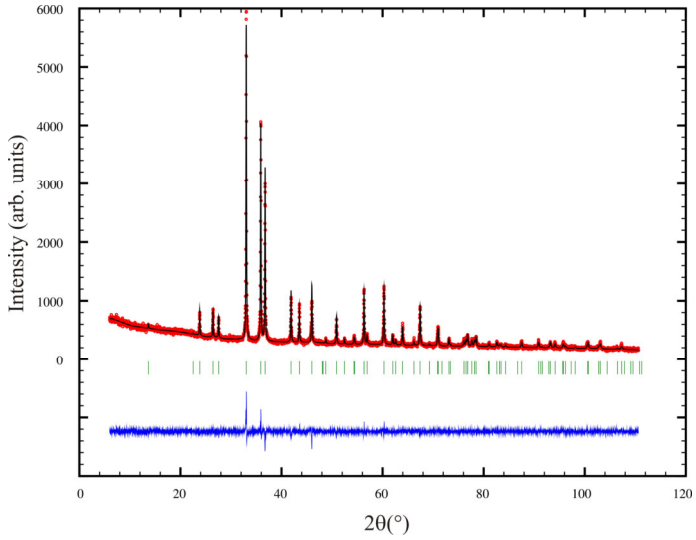


*a*

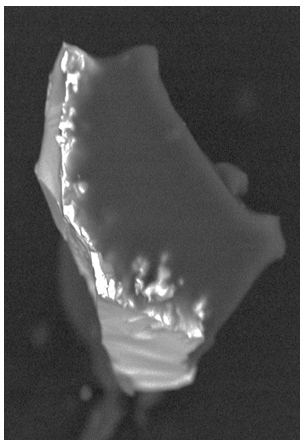

*b*

**Fig. 2** Experimental (circles), calculated (continuous line) and difference (lowest line) powder X-ray diffraction patterns (Stoe Stadi P, Cu $K\alpha_1$ radiation) (*a*) of sample $Nd_{0.33}Ni_{0.33}In_{0.20}Sn_{0.14}$ and scanning electron micrographs of a single crystal (*b*).

**Table 2** Crystal data and structure refinement for $NdNiIn_{0.6}Sn_{0.4}$.

| | |
|---|---|
| Empirical formula | $NdNiIn_{0.6}Sn_{0.4}$ |
| Molar mass ($g \cdot mol^{-1}$) | 319.3 |
| Crystal system | hexagonal |
| Space group | *P*-62*m* |
| Pearson symbol, *Z* | *hP*9, 3 |
| Unit-cell dimensions | $a = 0.74689(2)$ nm |
| | $c = 0.39483(1)$ nm |
| | $V = 0.190745(9)$ $nm^3$ |
| Radiation; λ, nm | Mo $K\alpha$; 0.071073 |
| Calculated density ($Mg \cdot m^{-3}$) | 8.3392 |
| Absorption coefficient ($mm^{-1} \cdot 10^6$) | 36.319 |
| $F(000)$, e | 412 |
| $\theta$ range for data collection | 3.15-41.06 |
| Range in *hkl* | $-13 \le h \le 13$, $-11 \le k \le 12$, $-6 \le l \le 7$ |
| Total no. reflections | 2939 |
| Independent reflections / parameters | 494/15 |
| Reflections with $I > 2\sigma(I)$ | 491 |
| Goodness-of-fit on $F^2$ | 1.45 |
| $R_1$ / $wR_2$ [$I > 2\sigma(I)$] | $R_1 = 0.0199$, $wR_2 = 0.0475$ |
| $R_1$ / $wR_2$ [all data] | $R_1 = 0.0202$, $wR_2 = 0.0477$ |
| Extinction coefficient | 237 |
| Largest diff. peak / hole ($e \cdot nm^{-3} \cdot 10^3$) | 1.45 / –1.43 |

**Table 3** Atomic coordinates and anisotropic displacement parameters for $NdNiIn_{0.6}Sn_{0.4}$.

| Atom | Wyckoff position | *x* | *y* | *z* | $U_{eq}$, nm$^2$ |
|---|---|---|---|---|---|
| Nd | 3*f* | 0.58650(5) | 0 | 0 | 0.0092(1) |
| Ni1 | 1*a* | 0 | 0 | 0 | 0.0122(3) |
| Ni2 | 2*d* | ⅓ | ⅔ | ½ | 0.0110(2) |
| *M** | 3*g* | 0.24907(6) | 0 | ½ | 0.0094(1) |
| Atom | | $U_{11}$, nm$^2$ | $U_{22}$, nm$^2$ | $U_{33}$, nm$^2$ | $U_{12}$, nm$^2$ [a] |
| Nd | | 0.0086(1) | 0.0102(1) | 0.0093(1) | 0.0051(1) |
| Ni1 | | 0.0130(4) | 0.0130(4) | 0.0106(6) | 0.0065(2) |
| Ni2 | | 0.0104(3) | 0.0104(3) | 0.0124(4) | 0.0052(1) |
| *M* [b] | | 0.0084(1) | 0.0088(2) | 0.0112(2) | 0.0044(1) |

[a] $U_{13} = U_{23} = 0$; [b] *M* = 0.6In + 0.4Sn

**Table 4** Interatomic distances ($\delta$, nm) and coordination numbers (CN) in the structure of $NdNiIn_{0.6}Sn_{0.4}$. All distances within the first coordination spheres are listed.

| Atom | | $\delta$, nm | CN | Atom | | $\delta$, nm | CN |
|---|---|---|---|---|---|---|---|
| Nd - | 4Ni2 | 0.29939(1) | 17 | *M* [a] - | 2Ni1 | 0.27125(3) | 12 |
| | 1Ni1 | 0.30884(4) | | | 2Ni2 | 0.28568(3) | |
| | 2*M* | 0.32014(5) | | | 2Nd | 0.32014(5) | |
| | 4*M* | 0.33393(4) | | | 2*M* | 0.32221(6) | |
| | 4Nd | 0.38985(2) | | | 4Nd | 0.33393(1) | |
| | 2Nd | 0.39483(1) | | | | | |
| Ni1 - | 6*M* | 0.27125(3) | 9 | Ni2 - | 3*M* | 0.28568(4) | 9 |
| | 3Nd | 0.30884(4) | | | 6Nd | 0.29939(1) | |

[a] *M* = 0.6In + 0.4Sn

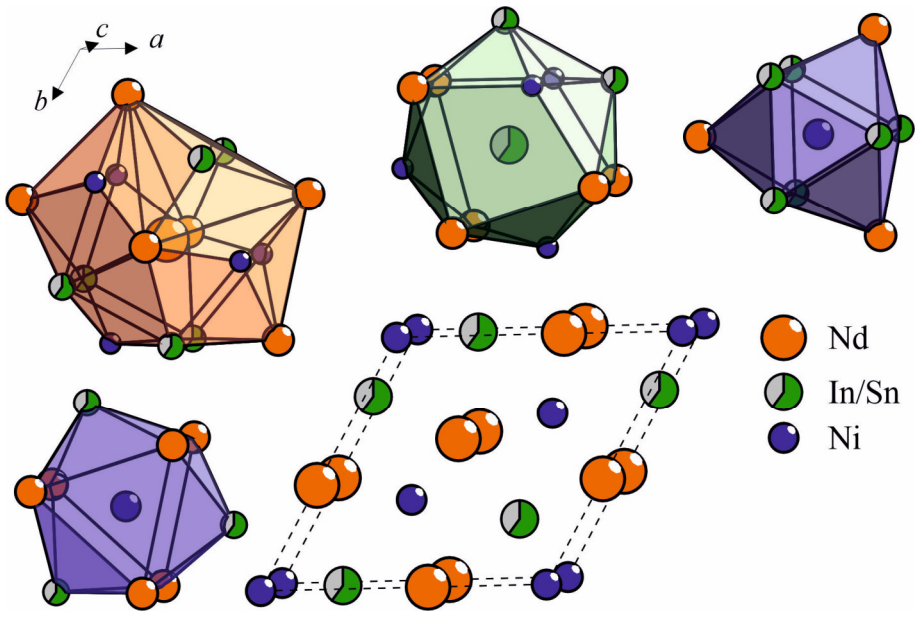


**Fig. 3** Projection of the structure of $NdNiIn_{0.6}Sn_{0.4}$ along the *c*-axis and coordination polyhedra of the atoms.

A comparison of the NdNiIn–NdNiSn system with the previously studied LaNiIn–LaNiSn and CeNiIn–CeNiSn systems [24] shows common trends in the nature of the interaction of the components: formation of limited substitutional solid solutions of different lengths with the structures of the boundary compounds. Approximately 13.5 at.% of indium is replaced by tin in the compounds with ZrNiAl-type

structures, while only 3.3 at.% of Sn is replaced by In in the compounds with TiNiSi-type structure. The results are influenced by structural features of the ZrNiAl and TiNiSi types. Similar situations may occur during the formation of $R_2T_2In_{1-x}M_x$ solid solutions ($R$ = La, Ce; $T$ = Ni, Cu; $M$ = Al, Sn) [25].

## 4. Conclusions

The existence of the limited solid solutions $NdNiIn_{1.0-0.6}Sn_{0-0.4}$ and $NdNiSn_{1.0-0.9}In_{0-0.1}$ with ZrNiAl-type structure, was observed at 870 K. Unit-cell parameters were determined. The crystal structure of the $NdNiIn_{0.6}Sn_{0.4}$ phase was refined using single-crystal diffraction: ZrNiAl-type, *P*-62*m*, *hP*9, $a$ = 0.74689(2); $c$ = 0.39483(1) nm, $R_1$ = 0.0202, $wR_2$ = 0.0477, 494 $F^2$ values, 15 variables.

## Acknowledgements

This work was supported by the Ministry of Education and Science of Ukraine under the grant No. 0124U000989. We are grateful to Prof. Dr. Thomas Doert and Lic. Cs. Eduardo Carrillo (both TU Dresden, Germany) for access to facilities and support during single-crystal data measurements, and to Rowena Wachtel (IFW Dresden, Germany) for help with the EDX analysis.

## References

[1] Ya.M. Kalychak, V.I. Zaremba, R. Pöttgen, M. Lukachuk, R.-D. Hoffmann, In: K.A. Gschneidner, Jr., J.-C. Bünzli, V.K. Pecharsky (eds.), *Handbook on the Physics and Chemistry of Rare Earth,* Vol. 34, Elsevier, Amsterdam, 2005, p. 1-133.

[2] A.E. Dwight, M.H. Mueller, R.A. Conner, J.W. Downey, H.W. Knott, *Trans. Metall. Soc. AIME* 242 (1968) 2075-2080.

[3] R. Ferro, R. Marazza, G. Rambaldi, *Z. Metallkd*. 65 (1974) 37-39.

[4] R.V. Skolozdra, In: K.A. Gschneidner, L. Eyring (eds.), *Handbook on the Physics and Chemistry of Rare Earths,* Vol. 24, Elsevier, Amsterdam, 1997, pp. 399-517.

[5] V.V. Romaka, L.P. Romaka, V.Ya. Krayovskyy, Yu.V. Stadnyk, *Stannides of Rare Earth and Transition Metals*, Lviv Polytech. Univ., 2015, 224 p., ISBN 978-617-607-816-6 (in Ukrainian).

[6] S. Gupta, K.G. Suresh, *J. Alloys Compd.* 618 (2015) 562-606.

[7] H. Oesterreicher, *J. Less-Common Met.* 30 (1973) 225-236.

[8] Ł. Gondek, J. Żukowski, M. Balanda, D. Kaczorowski, A. Szytuła, *Mater. Sci. Pol*. 26,4 (2008) 815-820.

[9] Ł. Gondek, A. Szytuła, D. Kaczorowski, Ya. Kalychak, B. Penc, J. Hernandes-Velasco, Yu. Tyvanchuk, *Chem. Met. Alloys* 1 (2008) 92-96.

[10] M. Sato, R.V. Denys, A.B. Riabov, V.A. Yartys, *J. Alloys Compd.* 397 (2005) 99-103.

[11] I.I. Bulyk, V.A. Yartys, R.V. Denys, Ya.M. Kalychak, I.R. Harris, *J. Alloys Compd.* 284 (1999) 256-261.

[12] Y. Öner, O. Kamer, J.H. Ross Jr., *J. Alloys Compd.* 460 (2008) 69-73.

[13] M. Kurisu, R. Hara, G. Nakamoto, Y. Andrh, S. Kawano, D. Schmitt, *Physica B* 312-313 (2002) 861-863.

[14] P. Palade, G. Principi, T. Spataru, P. Blaha, K. Schwarz, V. Kuncser, S. Lo Russo, S. Dal Toé, V.A. Yartys, *J. Radioanal. Nucl. Chem*. 266, 3 (2005) 553-556.

[15] A.B. Riabov, R.V. Denys, M. Sato, R.G. Delaplane, V.A. Yartys, *J. Alloys Compd.* 404-406 (2005) 107-111.

[16] O. Ardeleani, G. Blanitai, G. Filoti, P. Palade, *J. Phys.: Conf. Ser.* 182 (2009) 012045.

[17] W. Kraus, G. Nolze, *Powder Cell for Windows*, Berlin, 1999.

[18] STOE WinXPOW, Version 1.2, STOE & CIE GmbH. Darmstadt, 2001.

[19] J. Rodríguez-Carvajal, *Commission on Powder Diffraction (IUCr), Newsletter* 26 (2001) 12-19.

[20] V. Petříček, M. Dušek, L. Palatinus, *Z. Kristallogr.* 229 (2014) 345-352.

[21] P.I. Krypyakevych, V.Ya. Markiv, E.V. Mel'nyk, *Dopov. Akad. Nauk Ukr. RSR, Ser. A* (1967) 750-753.

[22] C. Brink Shoemaker, D.P. Shoemaker, *Acta Crystallogr.* 18 (1965) 900-905.

[23] K. Osamura, Y. Murakami, *J. Less-Common Met.* (1978) 60, 311-313.

[24] G. Nychyporuk, N. Dominyuk, I. Muts, A. Zelinskiy, R. Pöttgen, V. Zaremba, *Z. Naturforsch. B* 78 (2023) 427-433.

[25] N. Chumalo, V. Demchuk, G. Nychyporuk, V. Zaremba, *Visn. Lviv. Univ. Ser. Chem.* 51 (2010) 24-30.